

Mass relations of mirror nuclei with local correlations

C. Ma,¹ Y. Y. Zong,¹ Y. M. Zhao,^{1,2,*} and A. Arima^{1,3}

¹*Shanghai Key Laboratory of Particle Physics and Cosmology, School of Physics and Astronomy, Shanghai Jiao Tong University, Shanghai 200240, China*

²*Collaborative Innovation Center of IFSA (CICIFSA), Shanghai Jiao Tong University, Shanghai 200240, China*

³*Musashi Gakuen, 1-26-1 Toyotamakami Nerima-ku, Tokyo 176-8533, Japan*



(Received 2 June 2020; accepted 30 July 2020; published 26 August 2020)

In this paper we study mass relations of mirror nuclei, with our focus on local correlations of deviations between theoretical nuclear masses and experimental data. With inclusion of such local correlations, we are able to construct very accurate mass formulas of mirror nuclei. The root-mean-square deviation (RMSD) of our formulas is ~ 69 keV for nuclei with $10 \leq Z \leq 38$ and $Z > N + 1$ in the AME2016 database, and, furthermore, the RMSD value becomes only 51 keV if one excludes three experimental data for which experimental uncertainties are larger than 150 keV. More than 240 proton-rich nuclear masses with mass number A below 80 are predicted within the theoretical accuracy of 300 keV and are tabulated in the Supplemental Material of this paper. As a simple application, our predicted results are adopted to predict candidates with two-proton radioactivity.

DOI: [10.1103/PhysRevC.102.024330](https://doi.org/10.1103/PhysRevC.102.024330)

I. INTRODUCTION

Nuclear mass $M(N, Z)$ [where N is the neutron number and Z is the proton number] is a fundamental quantity in nuclear physics and astrophysics. Many theoretical models and approaches are developed to describe the state-of-the-art atomic-mass evaluation database and to predict unknown masses [1,2]. There are mainly two types of theoretical efforts, global models such as in Refs. [3–5], and local mass relations such as in Refs. [6–10].

In addition to these efforts, mass relations of mirror nuclei have been investigated in Refs. [11–13]. Here we mention that mass relations between mirror nuclei do present very accurate descriptions of atomic masses: Most theories yield typically deviations from experimental data 400–1000 keV for nuclei with neutron number $10 \leq Z \leq 38$ and $Z > N$, while the root-mean-square deviation (RMSD) in Ref. [12] is 398 keV and that in Ref. [13] is 120–290 keV (depending the value of $Z - N$); in Ref. [14], the RMSD is 110–130 keV for nuclei with $Z > N$ and mass number $A = 20$ –75. Mass relations of mirror nuclei are based on the assumption that nuclear interaction conserves the isospin symmetry, and with this assumption the mass difference of two mirror nuclei is given by the Coulomb interaction plus constant values related to the neutron-proton mass difference.

The main purpose of this paper is to report local correlations of deviations between theoretical nuclear masses and experimental data for mass relations of mirror nuclei, and with this correlation one is able to construct mass formulas with remarkable accuracy. The RMSD value of our formulas is ~ 69 keV for nuclei with $10 \leq Z \leq 38$ and $Z > N + 1$ in

the AME2016 database; and the RMSD value is reduced to only 51 keV if one excludes three experimental data for which experimental uncertainties are larger than 150 keV.

This paper is organized as follows. In Sec. II, we give an overview of previous mass relations of mirror nuclei, with a brief discussion of pairing correlation of Coulomb energies exhibited in our mass formulas; in Sec. III, we discuss local correlations of deviations between theoretical nuclear masses and experimental data and in Sec. IV adopt our predicted results to predict candidates of nuclei with $2p$ radioactive decay. We summarize our paper in Sec. V.

II. MASS RELATIONS OF MIRROR NUCLEI AND COULOMB ENERGY

As masses of mirror nuclei are connected dominantly via their Coulomb energies, it is useful to present a short review on studies of Coulomb energy in atomic nuclei. Assuming a spherical shape and uniform proton distribution with charge radius $R_c = r_0 A^{1/3}$, the Coulomb energy of a nucleus with given (N, Z, A) is as follows:

$$E_C = a_c \frac{Z^2}{A^{1/3}}, \quad a_c = \frac{3}{5} \frac{e^2}{4\pi\epsilon_0 r_0}, \quad (1)$$

where ϵ_0 is electric permittivity of vacuum and $a_c \simeq 0.72$ MeV if r_0 is taken to be 1.2 fm. By using this simple formula, we obtain mass difference between two mirror nuclei with $(N, Z) = (K - k, K)$ and $(K, K - k)$, denoted by $\delta_m(K - k, K) \equiv M(K - k, K) - M(K, K - k)$, as follows:

$$\begin{aligned} \delta_m(K - k, K) &= a_c k(2K - k)^{2/3} + k(m_p - m_n) \\ &= a_c \delta E_m + kC, \end{aligned} \quad (2)$$

*Corresponding author: ymzhao@sjtu.edu.cn

TABLE I. The parameters (a_c , C) and RMSD (σ) of Eqs. (2)–(4) for nuclei with $Z \geq 8$. These parameters are optimized by using the AME2016 [6] database, except for the ^{44}V nucleus whose mass is taken as in Ref. [15]. \mathcal{N} is the number of nuclei involved in parametrization.

δ	k	\mathcal{N}	a_c (MeV)	C (MeV)	σ (MeV)
δ_m	1	29	0.705(7)	-1.703(95)	0.121
	2	21	0.714(6)	-1.777(69)	0.124
	3	19	0.713(8)	-1.783(86)	0.204
	4	6	0.727(14)	-1.904(140)	0.149
δ_n		75	0.713(5)	-1.802(54)	0.114
δ_p		75	0.707(5)	-1.703(61)	0.117

where m_p (m_n) is mass of a hydrogen atom (a neutron), and we denote $\delta E_m = k(2K - k)^{2/3}$ while $C = m_p - m_n$. For brevity, we call Eq. (2) the δ_m relation. This relation was studied with both a_c and C taken as adjustable parameters depending on the value of k [13]. For the Atomic Mass Evaluation 2016 database (AME2016) [6] database for $10 \leq K \leq 38$ (except that the experimental mass value of ^{44}V in the AME2016 database is replaced by the latest value measured in Ref. [15]) as our inputs of $M(K - k, K)$, the resultant RMSD values (denoted by σ) are 121, 124, 204, and 149 keV for $k = 1-4$, respectively, as listed in the first four rows (corresponding to the δ_m) in Table I.

Similarly to Eq. (2), two new relations of mirror nuclei, called $\delta_n \equiv \delta_m(K - k, K) - \delta_m(K - k + 1, K)$ relation and $\delta_p \equiv \delta_m(K - k, K) - \delta_m(K - k, K - 1)$ relation, were suggested in Ref. [14]. Instead of two mirror nuclei involved in the δ_m relation, both the δ_n and δ_p relations involve masses of four nuclei. By using Eq. (2), one readily obtains

$$\delta_n(K - k, K) = a_c \delta E_n + (m_p - m_n) = a_c \delta E_n + C, \quad (3)$$

$$\delta_p(K - k, K) = a_c \delta E_p + (m_p - m_n) = a_c \delta E_p + C, \quad (4)$$

where $C = m_p - m_n$, as in Eq. (2); δE_n and δE_p originate from the Coulomb energy, and are given in the following form:

$$\delta E_n = k(2K - k)^{2/3} - (k - 1)(2K - k + 1)^{2/3}, \quad (5)$$

$$\delta E_p = k(2K - k)^{2/3} - (k - 1)(2K - k - 1)^{2/3}. \quad (6)$$

The key point of δ_p and δ_n relations is the same as that of Eq. (2), namely mass difference of two mirror nuclei is dominated by their Coulomb energies and the neutron-proton mass difference. The advantage of Eqs. (3) and (4) is that one does not need the total Coulomb energies E_C of two mirror nuclei but instead one needs only the Coulomb energy difference ΔE_C of two neighboring nuclei; as ΔE_C is always small, uncertainties originated from the evaluation of the Coulomb energy are expected to be small. The RMSDs are 114 and 117 keV for δ_n and δ_p , respectively, in the same region of the δ_m relation discussed above. Another advantage of the δ_p and δ_n relations is that parameters a_c and C are independent of k , which are much more convenient in extrapolations.

Clearly, the Coulomb energies in the above mass relations of mirror nuclei, δ_m , δ_p , and δ_n , are based on Eq. (1), in which nuclei are treated as uniformly charged, classical

electrostatic systems. However, atomic nuclei are very complex quantum systems of protons and neutrons. All even-even nuclei have spin zero in the ground states, which is a reflection of pairing correlation between like-nucleons in atomic nuclei. The Coulomb energy between protons is far weak to prevent pairing. On the other hand, the Coulomb energy depends on the spatial correlations, thus the odd-even feature of the Coulomb energy is a rough measure of pairing, as studied in Refs. [16–20]. To exemplify this pairing feature exhibited in Coulomb energy, we investigate the difference of δ_m for two neighboring nuclei with same k , namely $\delta_a(K - k, K) \equiv \delta M_m(K - k, K) - \delta M_m(K - 1 - k, K - 1)$. According to Eq. (2),

$$\delta_a(K - k, K) = a_c [k(2K - k)^{2/3} - k(2K - k - 2)^{2/3}]. \quad (7)$$

If one assumes $k \ll 2K$, then the above δ_a is reduced to

$$\delta_a(K - k, K) \simeq a_c \left(\frac{2^{5/3}}{3K^{1/3}} \right) k. \quad (8)$$

In this case the value of δ_a is proportional to k for given K .

In Fig. 1, we plot δ_a based on experimental masses (solid circles in black) and based on Eq. (8) (dashed lines), for $k = 1, 2, 3$. The parameter a_c for each k are optimized for the δ_m relation, shown in Table I. For $k = 1, 3$ cases, one sees an odd-even staggering of experimental-data-based δ_a with respect to the results given by Eq. (8). This feature is understood in terms of the seniority scheme for Coulomb interaction [18,21,22].

According to Refs. [21,22], the expectation of an arbitrary two-body interaction with respect to the lowest seniority ground state of an identical-particle system is given as follows:

$$V(j^n) = \tilde{V} + n\epsilon_j + \frac{n(n-1)}{2}\alpha + \left[\frac{n}{2} \right] \beta, \quad (9)$$

where j represents the angular momentum of a single-particle state in a schematic, single- j shell, and n is the number of valence particles ($n = Z - Z_0$, Z_0 is the magic number of the core). \tilde{V} represents the contribution of interactions within the full filled shells, and ϵ_j is the effective single-particle energy. The last two terms are derived from the interactions within the j shell, where α , β are quantities related to the two-body interaction matrix elements [22], and $[n/2]$ denotes the largest integer not greater than $n/2$.

Now we make use of Eq. (9) to calculate $\delta_a = M(K - k, K) - M(K - k - 1, K - 1) - M(K, K - k) + M(K - 1, K - k - 1)$. From Eq. (9), one derives the contributions from Coulomb interactions are as follows:

$$\begin{aligned} \delta_a(K - k, K) &= V(j^n) - V(j^{n-1}) - V(j^{n-k}) + V(j^{n-k-1}) \\ &= k\alpha + \frac{1 - (-1)^k}{2} (-1)^K \beta, \end{aligned} \quad (10)$$

where n , $n - 1$, $n - k$, and $n - k - 1$ are the valence proton numbers of corresponding nuclei involved in δ_a . This simple relation shows that there are two dominant parts in δ_a : One is approximately proportional to k and consistent with the feature exhibited in Eq. (8), and the other is an odd-even term which depends on the values of k and K .

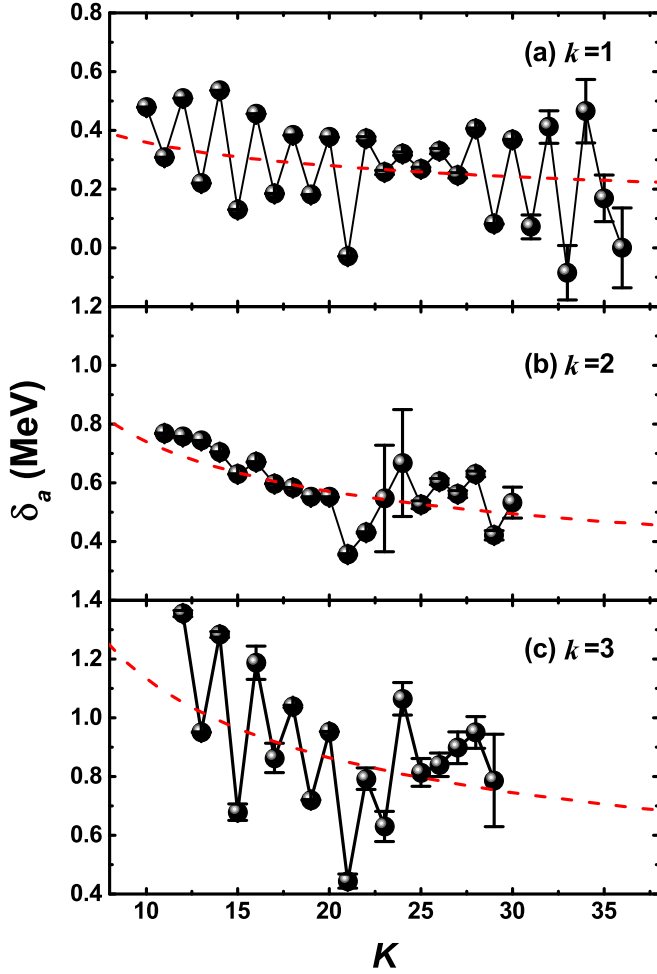


FIG. 1. Experimental and theoretical values of δ_a relation versus K . Panels (a), (b), and (c) correspond to $k = 1, 2$, and 3 , respectively. Experimental data (solid balls in black) are taken from the AME2016 database [6] except that of ^{44}V from Ref. [15]. Theoretical results, calculated by using Eq. (7), are plotted in dashed lines.

From Eqs. (2)–(4) and Eq. (10), we propose new mass relations as below.

$$\delta_m = a_c \delta E_m + kC + \frac{1 - (-1)^k}{2} \frac{k + (-1)^k}{2} \beta, \quad (11)$$

$$\delta_n = a_c \delta E_n + C + \frac{1 - (-1)^{K-k}}{2} \beta, \quad (12)$$

$$\delta_p = a_c \delta E_p + C + \frac{1 + (-1)^K}{2} \beta, \quad (13)$$

where E_m , E_n , and E_p are the same as in Eqs. (2)–(4).

As the odd-even feature of Coulomb energy is striking, the inclusion of odd-even term is expected to improve these formulas. Without details we note that the RMSD value of Eq. (11) becomes 112 and 192 keV for $k = 1$ and 3 , for which the RMSD is reduced by 9 and 12 keV, respectively, and the RMSD values of Eqs. (12) and (13) become 104 and 98 keV, respectively (the RMSD value reduced by 10 and 19 keV) if one includes one more parameter β as above.

Therefore, the odd-even feature is interesting, and the improvement with simple odd-even correction is not substantial. One has to resort more sophisticated correlations in order to refine the accuracy of predictions for mass relations of mirror nuclei.

III. MASS RELATIONS OF MIRROR NUCLEI WITH LOCAL CORRELATIONS

In the last section, we improved the relations of δ_m , δ_n , and δ_p by considering the odd-even term of Coulomb energy, originated from pairing correlation of protons. However, the value of β varies sizably in different shells. In order to make predictions as accurate as possible, evolution of β and shell effect should be considered. In this section, we report local correlation among deviations of δ_m , δ_n , and δ_p mass relations given in Eqs. (2)–(4), with respect to those extracted from experimental data.

To proceed our discussion, we define the deviations of theoretical δ values [δ_m , δ_n , and δ_p in Eqs. (2)–(4)] from δ values extracted from the AME2016 database [6] and denote these deviations D ,

$$D_m = \delta_m^{(\text{exp})} - a_c \delta E_m - C,$$

$$D_n = \delta_n^{(\text{exp})} - a_c \delta E_n - C,$$

$$D_p = \delta_p^{(\text{exp})} - a_c \delta E_p - C.$$

We note that the values of a_c and C in the above three definitions of D are optimized for Eqs. (2)–(4), respectively.

With this definition, we investigate the correlations between $D_m(K-3, K)$ and $D_m(K-1, K)$, $D_n(K-k, K)$ and $D_n(K-k, K-1)$, and $D_p(K-k, K)$ and $D_p(K-k+1, K)$. The correlated pair of D are so chosen that the values of β in Eq. (11)–(13) are canceled out, and in such cases the corresponding pair of D are expected to be correlated. In other words, these three correlations have considered the odd-even features in Eqs. (11)–(13) and further have considered the variations of β in different regions and shells, because correlated D values correspond to two neighboring nuclei with the same odd-even parity of Z and N .

Figure 2 plots such correlated D values, where linear correlation is seen. Therefore, we assume

$$D_m(K-k, K) = \lambda_m D_m(K-k+2, K), \quad (14)$$

$$D_n(K-k, K) = \lambda_n D_n(K-k, K-1), \quad (15)$$

$$D_p(K-k, K) = \lambda_p D_p(K-k+1, K), \quad (16)$$

where λ_m , λ_n , and λ_p are adjustable parameters. The red lines in Fig. 2 are plotted with optimized λ values. In Table II, we list optimized λ and Pearson correlation coefficient r which measures the degree of linear correlation between variables. The value of $r \sim 0.8$ corresponds to reasonably high linear correlation.

Now we investigate the accuracy of mass relations with such local correlation for the AME2016 database. The procedure to apply our mass formulas with local correlations is as follows. We first make use of Eqs. (2)–(4) and obtain

$$M^{(m)}(N, Z) = M(Z, N) + a_c \delta E_m(N, Z) + C, \quad (17)$$

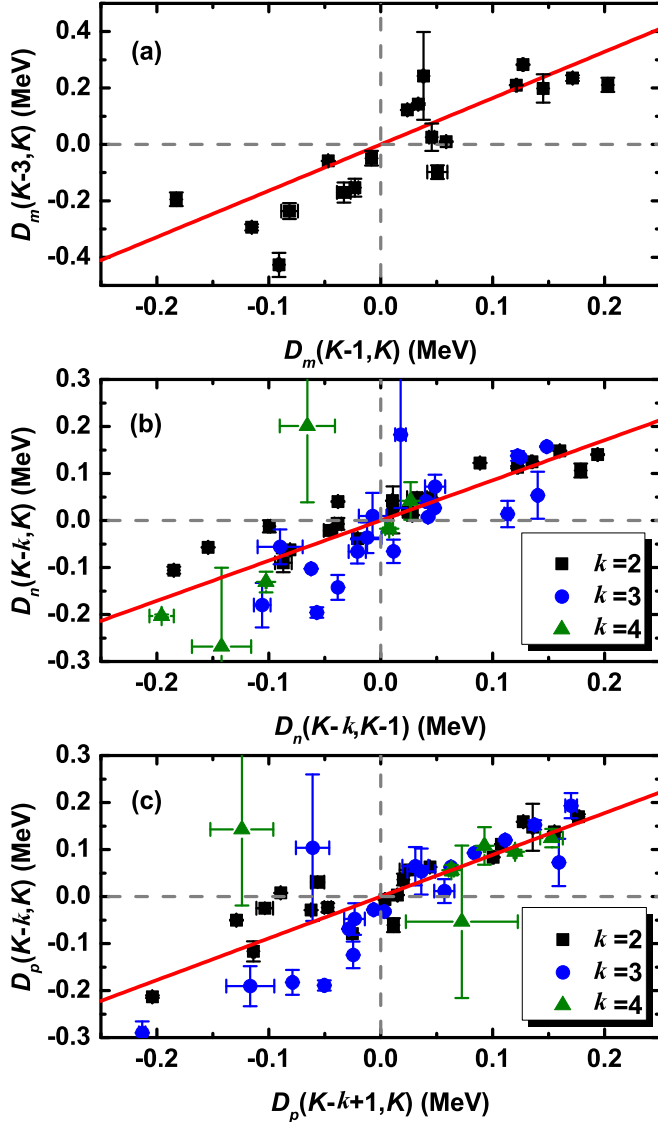


FIG. 2. Correlations between deviations between theoretical results and experimental data. The deviations are denoted by D_m , D_n , and D_p [defined in Eqs. (14), (15), and (16)], respectively, for δ_m , δ_n , and δ_p . (a) Correlation between $D_m(K-3, K)$ and $D_m(K-1, K)$, (b) correlation between $D_n(K-k, K)$ and $D_n(K-k, K-1)$, and (c) correlation between $D_p(K-k, K)$ and $D_p(K-k+1, K)$. The red lines are plotted by a slope $y = \lambda x$ and used to guide eyes. We put the error bars for cases which involves of large experimental uncertainties.

$$M^{(n)}(N, Z) = M(Z, N) + M(N+1, Z) - M(Z, N+1) + a_c \delta E_n(N, Z) + C, \quad (18)$$

$$M^{(p)}(N, Z) = M(Z, N) + M(N, Z-1) - M(Z-1, N) + a_c \delta E_p(N, Z) + C, \quad (19)$$

where predicted masses by using Eqs. (2)–(4) are denoted by a superscript “(m),” “(n),” “(p),” respectively. This step is the same as in Refs. [13,14]. We next considered the correction of

TABLE II. Linear correlation coefficient λ and RMSD (denoted by σ_{th}) of mass relations with correction of local correlations [namely by using Eqs. (20)–(22)] and Pearson correlation coefficient r for D [D_m , D_n , and D_p]. σ'_{th} is the same as σ_{th} but excluding three nuclei, ^{28}S , ^{40}Ti , and ^{55}Cu , whose experimental uncertainties are larger than 150 keV. The RMSD (denoted by σ_0) by using Eqs. (2)–(4) are presented for convenience.

D	λ	r	σ_0	$\sigma_{\text{th}}/\sigma'_{\text{th}}$ (MeV)
D_m	1.642	0.846	0.204	0.115/0.110
D_n	0.854	0.766	0.107	0.069/0.051
D_p	0.888	0.786	0.113	0.069/0.051

D , and our predicted mass is given by

$$M^{(\text{pred},m)}(N, Z) = M^{(m)}(N, Z) + D_m(N, Z), \quad (20)$$

$$M^{(\text{pred},n)}(N, Z) = M^{(n)}(N, Z) + D_n(N, Z), \quad (21)$$

$$M^{(\text{pred},p)}(N, Z) = M^{(p)}(N, Z) + D_p(N, Z). \quad (22)$$

Let us denote the RMSD values by using Eqs. (2)–(4) by σ_0 , and those of Eqs. (20)–(22) by σ_{th} . Our numerical experiments show that the value of σ_{th} by using Eq. (20) is 115 keV for $k=3$, while the corresponding σ_0 is 204 keV (without the correction of local correlation as above). Very remarkably, one obtains that σ_{th} by using Eqs. (21)–(22) for $k=2-4$ are 69 keV, in comparison with the RMSD values, 107 keV and 113 keV, for Eqs. (3) and (4), respectively.

It is worthy to note that experimental mass uncertainties of ^{28}S , ^{40}Ti , and ^{55}Cu are larger than 150 keV; if we exclude experimental masses values of those three nuclei from our numerical calculations, Eqs. (20)–(22) are even more accurate: the RMSD values using Eqs. (20)–(22) with those three nuclei excluded, denoted by σ' in Table II, are 110, 51, and 51 keV, respectively.

These RMSD values of Eqs. (20)–(22) are by far smaller than those of any other methods in the market, either global approaches such as the DZ28 [3], FRDM12 [4], and WS4 [5], the RMSD values of which are 451, 996, and 406 keV, respectively, and local relations of generalized Garvey-Kelson mass formulas [12], the RMSD value of which is 398 keV, in comparison with the AME2016 database [13], for the same set of nuclei.

It is of interest to investigate the predictive power of our formulas with corrections of local correlation, and here we use Eqs. (21) and (22). This is exemplified by an extrapolation from the AME1995 database [23] to the AME2016 database. The procedure of our extrapolation is as follows:

- (i) The parameters a_c and C in Eqs. (3) and (4) and λ in Eqs. (15) and (16) are optimized by using the AME1995 [23];
- (ii) By using the optimized values of a_c and C , we obtain our preliminary values of predicted masses by using Eq. (18) and/or Eq. (19), denoted by $M^{(n)}(N, Z)$ and/or $M^{(p)}(N, Z)$, respectively;
- (iii) Next we calculate D_n and D_p , and optimize the value of λ ;

TABLE III. The results of extrapolation from AME1995 database [23] to AME2016 database [6]. The values under ‘‘Expt.’’ are taken from the AME2016 database, except for ^{44}V taken from Ref. [15]; ‘‘A-W’’ corresponds to the Audi-Wapstra extrapolation in the AME1995 database [23]; ‘‘Ref. [14]’’ corresponds to predicted results by using the δ_n and δ_p relations, i.e., Eqs. (3) and (4) in this paper; and the column ‘‘This work’’ corresponds to predicted results by using Eqs. (21) and (22), proposed in this paper. In the last row we list the RMSDs in comparison with results in the AME2016 database. All values are in units of MeV.

Nuclei	Expt.	A-W	Ref. [14]	This work
^{41}Ti	-15.698(28)	-15.713(35)	-15.634(75)	-15.625(75)
^{43}V	-17.916(43)	-18.024(233)	-17.657(89)	-17.793(89)
^{44}V	-23.827(20)	-23.846(84)	-23.687(76)	-23.805(76)
^{45}Cr	-19.515(35)	-19.412(102)	-19.415(87)	-19.482(87)
^{47}Mn	-22.566(32)	-22.263(158)	-22.454(90)	-22.527(90)
^{48}Mn	-29.296(7)	-28.997(71)	-29.226(77)	-29.301(77)
^{49}Fe	-24.751(24)	-24.582(158)	-24.641(95)	-24.676(95)
^{51}Co	-27.342(48)	-27.274(149)	-27.318(96)	-27.338(96)
^{52}Co	-34.361(8)	-33.916(65)	-34.351(76)	-34.376(76)
^{53}Ni	-29.631(25)	-29.379(158)	-29.645(92)	-29.607(92)
^{55}Cu	-31.635(156)	-31.624(298)	-31.699(94)	-31.715(94)
^{56}Cu	-38.643(15)	-38.601(140)	-38.617(76)	-38.580(76)
RMSD	—	0.204	0.106	0.058

- (iv) With optimized λ , we readily calculate D values to be adopted in our extrapolation, namely from $D_n(K-k, K-1)$ to $D_n(K-k, K)$ or from $D_n(K-k+1, K)$ to $D_n(K-k, K)$;
- (v) $M^{(\text{pred})}$ are calculated by using Eqs. (21) and (22).
- (vi) Our predicted mass values are taken to be the uncertainty-weighted average of $M^{(\text{pred})}$.
- (vii) Evaluation of theoretical uncertainties for predicted masses follow the same procedure as in previous studies, e.g., Refs. [8,14].

In Table III and Fig. 3, we present our predicted the masses of 12 nuclei, which were not accessible in the AME1995 database [23] but compiled in the AME2016, with $k = 2, 3, 4$. For comparison we also present the predicted results of Audi-Wapstra extrapolation (denoted A-W) in the AME1995 database and those predicted in Ref. [14]. The RMSD values with respect to the AME2016 database are listed in the last row of Table III (we note that we replace the mass of the ^{44}V nucleus in the AME2016 database by that in a recent experimental measurement [15]). Clearly, our predicted masses are, in general, the most competitive; our RMSD value of our extrapolated results for these nuclei is below 60 keV.

Encouraged by the remarkable agreement between our predicted results with experimental data, here we also predict the three experimental data (^{28}S , ^{40}Ti , and ^{55}Cu) for which uncertainties are larger than 150 keV, based on other data compiled in the AME2016 database (the result for ^{44}V is replaced by that in Ref. [15]). Our theoretical mass excesses of ^{28}S , ^{40}Ti and ^{55}Cu [whose experimental mass excesses of ^{28}S , ^{40}Ti , and ^{55}Cu are 4073 (160) keV, -8850(160) keV, and -31635(156) keV, respectively] are 4205(86) keV, -9105(84) keV, and

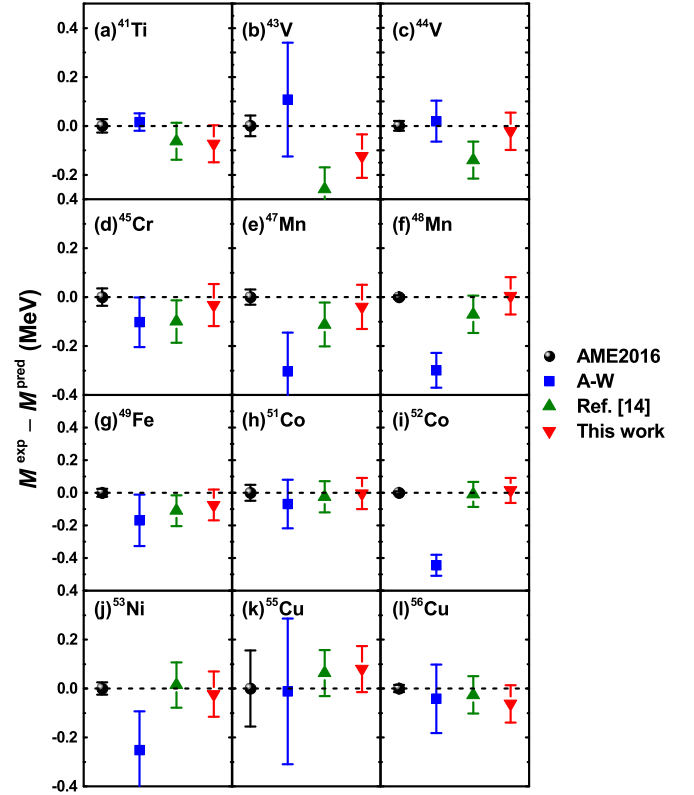


FIG. 3. Deviations between experimental masses (denoted by ‘‘AME2016,’’ solid balls in black) and predicted values in the AME1995 database (denoted by ‘‘A-W,’’ solid squares in blue) [23], predicted values by Ref. [14] (denoted by ‘‘Ref. [14],’’ solid up-triangles in green), and predicted values by using Eqs. (21) and (22) in this work (denoted by ‘‘This work,’’ down-triangles in red). The experimental mass of ^{44}V is taken from Ref. [15]. One sees that our predicted results for these nuclei agree best with experimental data. Panels (a)–(l) correspond to the same 12 nuclei listed in Table III.

-31798 (82) keV, respectively. As a by-product of this paper, we enclose of our predictions of totally 244 proton-rich nuclear masses which are experimentally inaccessible at present, for mass number $21 \leq A \leq 81$ and theoretical uncertainties below 300 keV, in the Supplemental Material of this paper [24].

IV. PREDICTION OF TWO-PROTON RADIOACTIVITY AND PROTON DRIP LINES

Because nuclei studied in this paper are of proton-rich type, and because our formulas are very accurate, one immediate application of our extrapolated nuclear masses is to discuss candidates of two-proton ($2p$) radioactivity, which has drawn enormous attention in recent years. We define p and $2p$ decay energies as follows:

$$Q_p(N, Z) = M(N, Z) - M(N, Z-1) - M_p, \quad (23)$$

$$Q_{2p}(N, Z) = M(N, Z) - M(N, Z-2) - 2M_p. \quad (24)$$

One requirement of $2p$ radioactivity for given nucleus is its $Q_p < 0$, and meanwhile $Q_{2p} > 0$. Among proton-rich nuclei of our predicted mass database (see the Supplemental

TABLE IV. Predicted two-proton decay energy Q_{2p} , one-proton decay energy Q_p , and half-life $T_{1/2}$ for a number of candidates with $2p$ radioactivity.

Nuclei	Q_{2p} (MeV)	Q_p (MeV)	$\log_{10} T_{1/2}$ (s) [32]
^{34}Ca	2.152(118)	-0.203(151)	-11.44 $^{+0.38}_{-0.35}$
^{38}Ti	2.764(142)	-0.124(168)	-11.98 $^{+0.34}_{-0.32}$
^{39}Ti	0.939(127)	-0.159(151)	-2.77 $^{+1.66}_{-1.35}$
^{42}Cr	0.964(173)	-0.895(198)	-1.33 $^{+2.44}_{-1.86}$
^{59}Ge	1.242(175)	-0.045(199)	1.70 $^{+2.09}_{-1.69}$
^{66}Kr	2.929(244)	-0.021(256)	-5.74 $^{+0.85}_{-0.75}$
^{70}Sr	3.385(268)	-0.076(280)	-6.24 $^{+0.78}_{-0.70}$
^{71}Sr	2.171(242)	-0.179(257)	-1.61 $^{+1.42}_{-1.20}$

Material), there have been five nuclei, ^{19}Mg , ^{45}Fe , ^{48}Ni , ^{54}Zn , and ^{67}Kr , that have been reported to have $2p$ radioactivity in Refs. [25–31]. Their experimental $2p$ decay energies Q_{2p}^{exp} are 0.750(50) [6,30], 1.154(16) [6,29], 1.305(37) [6], 1.480(20) [6,28], and 1.690(17) [31] MeV, respectively. The corresponding theoretical values based on the extrapolation of this work are 0.819(92), 1.198(202), 1.384(234), 1.600(178), and 1.574(215) MeV. One sees that our predicted Q_{2p} are quite close to these experimental values, although we extend our predictions from $k \leq 4$ to $k = 5-8$.

In addition to these experimentally known $2p$ -radioactive nuclei, it is interesting to search other candidates which satisfy $Q_p < 0$ and $Q_{2p} > 0$. For convenience, we also present a rough estimation of half-lives for these candidates by using an empirical formula suggested in Ref. [32],

$$\log T_{1/2} = [(a \times l) + b] \frac{(Z - 2)^{0.8}}{\sqrt{Q_{2p}}} + [(c \times l) + d], \quad (25)$$

where the values of a , b , c , d are 0.1578, 1.9474, -1.8795, and -24.847, respectively. $T_{1/2}$ is the half-life of $2p$ radioactivity in unit of second, Q_{2p} is in unit of MeV, and l is the orbital angular momentum carried by the protons and set to zero by the spin-parity selection rule [33].

Based on the database of Supplemental Material in this paper, eight candidate nuclei, ^{34}Ca , ^{38}Ti , ^{39}Ti , ^{42}Cr , ^{59}Ge , ^{66}Kr , ^{70}Sr , ^{71}Sr , have their $2p$ -radioactive half-lives below 100 s and thus might be suitable for experimental observation of $2p$ radioactive decay. For convenience, our predicted Q_{2p} , Q_p , and $\log T_{1/2}$ are listed in Table IV. Interestingly, the first five candidates are also predicted in Ref. [33].

In Fig. 4 we show the predicted proton and diproton drip lines based on the calculation of this work. The eight $2p$ -radioactive candidates that we predict in this paper are denoted in red, and those five nuclei which were experimentally suggested to have $2p$ radioactivity are denoted in purple. The proton drip line is plotted where two isotones satisfying $Q_p(N, Z) < 0$ and $Q_p(N, Z + 1) > 0$ with largest Z , while the diproton drip line is plotted where two isotones satisfying $Q_{2p}(N, Z) < 0$ and $Q_{2p}(N, Z + 1) > 0$ with smallest Z . Thus $2p$ -radioactive candidates are expected to locate between these two lines. We note that ^{54}Zn locates outside the drip

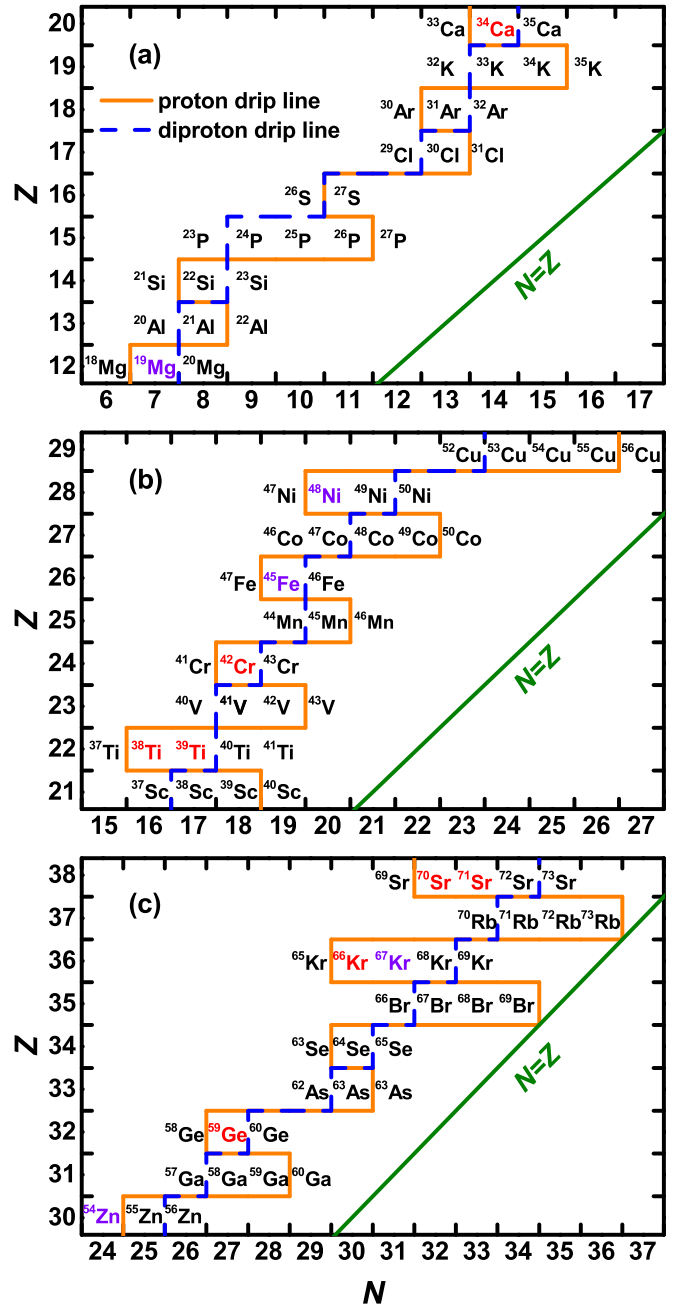


FIG. 4. The predicted proton and diproton drip lines based on predicted masses in this work. (a) $12 \leq Z \leq 20$, (b) $21 \leq Z \leq 29$, and (c) $30 \leq Z \leq 38$. Nuclear symbols in red are predicted here to be candidates with $2p$ radioactivity, and those in purple have been experimentally suggested to have $2p$ radioactivity (and are consistent with predictions in this work).

lines, whereas the predicted $Q_p(24, 30) = -28 \pm 225$ keV, which is quite close to 0 and may not affect its $2p$ radioactivity according to our extrapolation.

V. SUMMARY

To summarize, in this paper we study mass relations of mirror nuclei with local correlations. We revisit the odd-even

staggering of Coulomb energy and introduce correlations of deviations between experimental data and our mass relations. With considering this correlation, we are able to construct formulas with the RMSD values below 70 keV; furthermore, if we exclude three experimental data of three nuclei, ^{28}S , ^{40}Ti , and ^{55}Cu , whose mass uncertainties are larger than 150 keV, the RMSD of our formulas is only 51 keV.

We demonstrate the strong predictive power of our formulas by numerical experiment. We predict masses in the region of our interest based on the AME1995 database [23] and compare our predicted results with those in the AME2016. The RMSD of our predicted results, which are available in the AME2016 database but not accessible in the AME1995 database [23], is remarkably small (58 keV).

We predict more than 240 masses of proton-rich nuclei with proton number from 10 to 44, with the requirement of uncertainties below 300 keV, and enclose them in the Supplemental Material of this paper. As a by-product of these predictions, we predict one-proton and two-proton drip lines in the same region and candidates with $2p$ radioactivity.

ACKNOWLEDGMENTS

We thank the National Natural Science Foundation of China (Grants No. 11975151, No. 11675101, and No. 11961141003) and MOE Key Lab for Particle Physics, Astrophysics and Cosmology for financial support.

-
- [1] D. Lunney, J. M. Pearson, and C. Thibault, *Rev. Mod. Phys.* **75**, 1021 (2003).
- [2] K. Blaum, *Phys. Rep.* **425**, 1 (2006).
- [3] J. Duflo and A. P. Zuker, *Phys. Rev. C* **52**, R23 (1995).
- [4] P. Möller, W. D. Myers, H. Sagawa, and S. Yoshida, *Phys. Rev. Lett.* **108**, 052501 (2012).
- [5] N. Wang, M. Liu, X. Z. Wu *et al.*, *Phys. Lett. B* **734**, 215 (2014).
- [6] W. J. Huang, G. Audi, M. Wang *et al.*, *Chin. Phys. C* **41**, 030002 (2017); M. Wang, G. Audi, F. G. Kondev *et al.*, *ibid.* **41**, 030003 (2017).
- [7] G. T. Garvey and I. Kelson, *Phys. Rev. Lett.* **16**, 197 (1966); G. T. Garvey, W. J. Gerace, R. L. Jaffe *et al.*, *Rev. Mod. Phys.* **41**, S1 (1969).
- [8] G. J. Fu, H. Jiang, Y. M. Zhao, S. Pittel, and A. Arima, *Phys. Rev. C* **82**, 034304 (2010); G. J. Fu, Y. Lei, H. Jiang, Y. M. Zhao, B. Sun, and A. Arima, *ibid.* **84**, 034311 (2011).
- [9] H. Jiang, G. J. Fu, B. Sun *et al.*, *Phys. Rev. C* **85**, 054303 (2012).
- [10] I. Kelson and G. T. Garvey, *Phys. Lett.* **23**, 689 (1966).
- [11] J. Jänecke, *Phys. Rev. C* **6**, 467 (1972).
- [12] J. L. Tian, N. Wang, C. Li, and J. Li, *Phys. Rev. C* **87**, 014313 (2013).
- [13] M. Bao, Y. Lu, Y. M. Zhao, and A. Arima, *Phys. Rev. C* **94**, 044323 (2016).
- [14] Y. Y. Zong, M. Q. Lin, M. Bao, Y. M. Zhao, and A. Arima, *Phys. Rev. C* **100**, 054315 (2019).
- [15] Y. H. Zhang, P. Zhang, X. H. Zhou, M. Wang, Y. A. Litvinov, H. S. Xu *et al.*, *Phys. Rev. C* **98**, 014319 (2018).
- [16] J. A. Nolen and J. P. Schiffer, *Annu. Rev. Nucl. Sci.* **19**, 471 (1969).
- [17] E. Feenberg and G. Goertzel, *Phys. Rev.* **70**, 597 (1946).
- [18] B. C. Carlson and I. Talmi, *Phys. Rev.* **96**, 436 (1954).
- [19] S. Sengupta, *Nucl. Phys.* **21**, 542 (1960).
- [20] J. Jänecke, *Z. Phys.* **196**, 477 (1966).
- [21] I. Talmi, *Rev. Mod. Phys.* **34**, 704 (1962).
- [22] R. D. Lawson, *Theory of the Nuclear Shell Model* (Clarendon Press, Oxford, 1980).
- [23] G. Audi and A. H. Wapstra, *Nucl. Phys. A* **595**, 409 (1995).
- [24] See Supplemental Material at <http://link.aps.org/supplemental/10.1103/PhysRevC.102.024330> for predicted mass excesses for 244 proton-rich nuclear masses which are experimentally unaccessible at present for mass number $21 \leq A \leq 81$ and theoretical uncertainties below 300 keV.
- [25] M. Pfützner, E. Badura, C. Bingham *et al.*, *Eur. Phys. J. A* **14**, 279 (2002).
- [26] M. Pfützner, M. Karny, L. V. Grigorenko, and K. Riisager, *Rev. Mod. Phys.* **84**, 567 (2012).
- [27] J. Giovinazzo, B. Blank, M. Chartier, S. Czajkowski, A. Fleury, M. J. Lopez Jimenez, M. S. Pravikoff, J. C. Thomas, F. de Oliveira Santos, M. Lewitowicz, V. Maslov, M. Stanoiu, R. Grzywacz, M. Pfützner, C. Borcea, and B. A. Brown, *Phys. Rev. Lett.* **89**, 102501 (2002).
- [28] B. Blank, A. Bey, G. Canchel, C. Dossat, A. Fleury, J. Giovinazzo *et al.*, *Phys. Rev. Lett.* **94**, 232501 (2005).
- [29] C. Dossat, A. Bey, B. Blank, G. Canchel, A. Fleury, J. Giovinazzo *et al.*, *Phys. Rev. C* **72**, 054315 (2005).
- [30] I. Mukha, K. Sümmerer, L. Acosta, M. A. G. Alvarez, E. Casarejos, A. Chatillon *et al.*, *Phys. Rev. Lett.* **99**, 182501 (2007).
- [31] T. Goigoux, P. Ascher, B. Blank *et al.*, *Phys. Rev. Lett.* **117**, 162501 (2016).
- [32] I. Sreeja and M. Balasubramaniam, *Eur. Phys. J. A* **55**, 33 (2019).
- [33] J. P. Cui, Y. H. Gao, Y. Z. Wang, and J. Z. Gu, *Phys. Rev. C* **101**, 014301 (2020).